The New Generation of Cryogenic Liquid-Fueled Medium-Lift Launch Vehicle

CHEN Xiaofei[1], YU Long[1], YUAN He[1], ZHAO Yongzhi[1], SONG Zhengyu[2*], ZHANG Tao[2]

1 Beijing Institute of Astronantical Systems Engineering, Beijing 100076
2 China Academy of Launch Vehicle Technology, Beijing 100076

Abstract: The maiden flight of LM-8 performed perfectly on December 22, 2020. The design concept of modularization, seriation and combination has been perfectly exhibited in LM-8. The four main technical innovations, including rapid integrated design based on modularization, engine thrust regulation, modal parameters acquisition technology based on numerical simulation, and flight load control, were verified during the maiden flight. LM-8 is now positioned to be the main force in China's medium launch vehicles for commercial launch. In the future, the mission adaptability of LM-8 will be improved to provide efficient and low-cost launch services. In addition, new technologies to allow repeated use and autonomous flight will be validated.

Key words: LM-8, modularization, thrust regulation, dynamic characteristics, load control

1 INTRODUCTION

The development of the new generation of cryogenic liquid-fueled medium-lift launch vehicle, LM-8, was approved by China National Space Administration (CNSA) in 2017. It was developed by the China Academy of Launch Vehicle Technology, which is a subsidiary of CASC, with the following expectation:

1) Demand for spacecraft launches continues to rise

The number of satellites in orbit globally exceeded 3,000 as of the end of 2020. From 2018 to 2020, the number of global launch vehicle launches exceeded 100 per year. It indicated that since the end of the Cold War, the global demand for space launches has been constantly increasing, and a wave of world space development is coming. According to the Satellite Manufacturing and Launch Global Market Analysis Report[1] released by Euroconsult in the past three years, the demand for launching 1—8 t spacecrafts has continued to rise, of which the number of satellites whose target orbits are SSO and LEO accounts for 59%. In the field of commercial space, constellation networking has become a major theme, with high-efficiency, responsive, and low-cost entry into space as the main requirement. The Long March series launch vehicle in service at that time could generally only undertake launches of spacecraft of 1—3 t for SSO missions. However, at the same time, they are not economical to meet the launch requirements for the low orbit satellite constellations. There was an obvious gap between the requirements and the carrying capacity.

2) Perfecting the family of the new generation launch vehicles (NGLVs) [2]

According to the original planning of the NGLVs in China, the large-lift launch vehicle LM-5, the small-lift launch vehicle LM-6, and the medium-lift launch vehicle LM-7, were developed one by one. However, due to their different target locations and missions, these three launch vehicles were not cost-effective for the launch of SSO satellites with a weight about 3−4.5 t.

3) Provide more environmentally-friendly launch vehicles

Using environmentally-friendly propellants is the development trend of today's launch vehicles. International mainstream launch vehicles all use environmentally-friendly propellants, with the exception of the Proton launch vehicle where it was announced that it is due to be decommissioned before 2025. China pays more and more attention to environmental protection initiatives, and has proposed 'developing an environment-friendly society' at the 19th National Congress of the Communist Party of China. It is essential to promote the pollution-free development of launch vehicles. So LM-8 adopted green propellants, which is an important feature of the new generation launch vehicles.

Based on the above background, the LM-8 project was initiated. After a three-year development period, the LM-8 launch vehicle took off from the Wenchang Spacecraft Launch Site on December 22, 2020. The flight sequence of more than 1,500 s and a series of separations successfully resulted in 5 satellites accurately inserted into their predetermined target orbits. The maiden flight of LM-8 performed perfectly.

2 OVERVIEW OF LM-8

2.1 Configuration of LM-8

The LM-8 launch vehicle contains a two-stage structure with two side first-stage boosters, giving an overall total length of 50.3 m, a lift-off thrust of about 4752 kN, providing a lift-off mass of about 356 t. The general layout is shown in Figure 1.

The first stage, with a diameter of 3.35 m, has 2 liquid oxygen/kerosene engines with thrust of 1188×2 kN. The second stage, with a diameter of 3 m, has 2 liquid oxygen/liquid hydrogen engines with a thrust of 164 kN. Each of the two side boosters, with a diameter of 2.25 m, have 1 liquid oxygen/kerosene engine with a thrust of 1188 kN. The diameter of the fairing is 4.2 m.
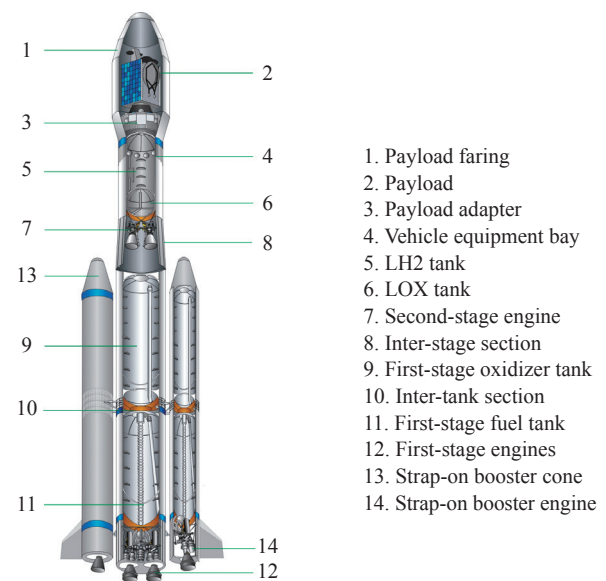

Figure 1 Layout of LM-8

1. Payload faring
2. Payload
3. Payload adapter
4. Vehicle equipment bay
5. LH2 tank
6. LOX tank
7. Second-stage engine
8. Inter-stage section
9. First-stage oxidizer tank
10. Inter-tank section
11. First-stage fuel tank
12. First-stage engines
13. Strap-on booster cone
14. Strap-on booster engine

LM-8 consists of a number of subsystems: aerostructure, propulsion, control, telemetry, Reaction Control System (RCS), trajectory measurement & safety sub-systems. The main technical parameters of the LM-8 are shown in Table 1.

Table 1 Technical parameters of LM-8

Stage	Booster	1st stage	2nd stage
Stage diameter (m)	2.25	3.35	3.00
Stage length (m)	26.8	27.8	12.375
Mass of propellants (t)	72×2	156	18.2
Propellant	LOX/KO	LOX/KO	LOX/LH2
Engine	YF-100	YF-100	YF-75
Engine thrust (kN)	1188	1188×2	82.7×2
Engine specific impulse (N•Sec/kg)	2942	2942	4312
Numbers of boosters	2		
Lift-off mass (t)	356		
Overall length (m)	50.34		
Fairing diameter (m)	4.20		
Fairing length (m)	12.6		
700 km SSO launch capability (kg)	5000		

2.2 Capability of LM-8

LM-8 is capable of carrying out mainstream LEO, GTO and SSO missions. The carrying capacity into LEO is more than 8 t. A satellite which is less than 2.8 t can be launched into GTO. The carrying capacity for SSO at different orbital altitudes is shown in Table 2.

Table 2 LM-8 carrying capacity for SSO mission at different altitudes

Altitude (km)	Capacity (kg)
500	5500
600	5250
700	5000
800	4750
900	4500
1000	4250
1100	4000

2.3 Diverse Satellite Layouts

LM-8 has two fairing configurations with the same diameter of 4.2 m but of different lengths, which can be adapted for various satellites.

LM-8 provides diverse standard adapter interfaces, including international standard payload adapters, such as 660 mm, 937 mm, 1194 mm clamp-band interfaces. In addition, a variety of explosive bolt devices are available, which are very flexible for small satellites.

Based on the available envelope of the fairing, multi-layer and multi-direction satellite layouts were proposed for LM-8 missions, as shown in Figure 2. To ensure multi-satellite separation collision avoidance, different separation sequences and directions are established.
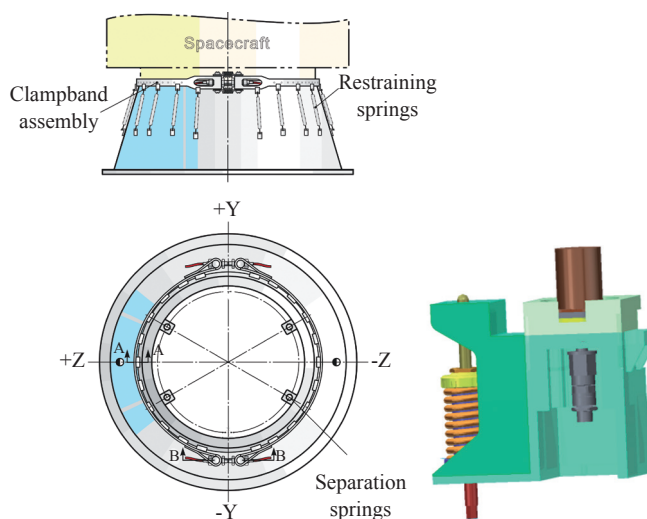

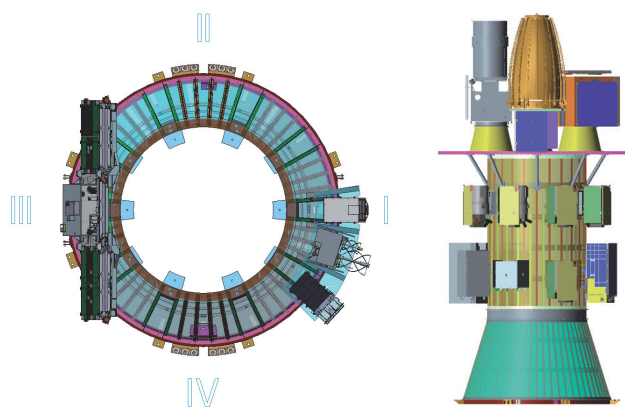Figure 2 Diverse standard adapter interfaces

Figure 3 Multi-satellite layout

3 THE TECHNICAL INNOVATIONS AND FLIGHT PERFORMANCE OF LM-8

The engineering development of the LM-8 project followed the concept of modularization, seriation, and combination. LM-8 fully inherited the modules and technologies from in-service launch vehicles and took full advantage of the proven test-
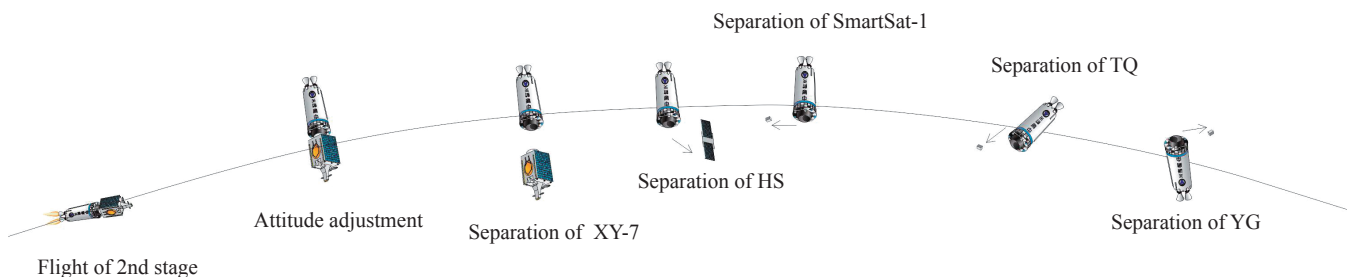

Figure 4 Separation sequences of the maiden flight of LM-8

ing results and technologies to accomplish its rapid integrated development. However, new requirements such as lack of load capacity due to inherited modules, matching the interfaces of modules which were originally designed for other rockets, and so on had to be overcome. Based on the existing module combination, a reverse design approach for LM-8 was initiated to complete the integrated development at the most economical cost and in the shortest period. Due to the constraints arising from the existing modules, multiple innovative technologies such as engine throttling, wind compensation trajectory design, active load relief, and load refinement design were adopted.

There were four main technical characteristics in the development of LM-8, including rapid integration design based on modularization[4], engine thrust regulation, dynamic characteristic acquisition based on numerical simulation, and onboard load relief control, which were verified during the maiden flight.

3.1 Rapid Integration Design Based on Modularization

The development process is shown in Figure 5. The first step was to determine the design constraints using inherited modules. The second step was to carry out an overall design based on the constraints. The third step was a module interface design. The fourth step was an iterative verification for the above steps.

3.1.1 Determination of design constraints

The required design performance of LM-8 for SSO was more than 4.5 t. According to the load bearing capacity of the structural module, iterative analysis was carried out to obtain the load design conditions. The structure to enable the ultimate load capacity was determined by examining the comprehensive effects of axial load, bending moment load, tank pressure and so on. The axial load and tank pressure were relatively fixed in flight, while the bending moment load was positively related to the flight $Q\alpha$ value (flight dynamic pressure multiplied by flight angle of attack). Therefore, the $Q\alpha$ value could be reduced through the following joint optimization of trajectory and attitude control, so as to reduce the flight load and meet the structural load requirements. The process of determination of design constraints is shown in Figure 6.

The maximum overload constraint in flight was determined according to the adaptability of mainstream satellites, because the maximum overload mainly impacts the static load of the satellites. The larger the maximum overload, the higher the static load of the satellites. Using statistics, as shown in Table 3, the maximum overload of most China's launch vehicles is less than 6 g, while LM-2C and LM-2D have a maximum overload of more than 6 g. However, the satellites launched by LM-2C
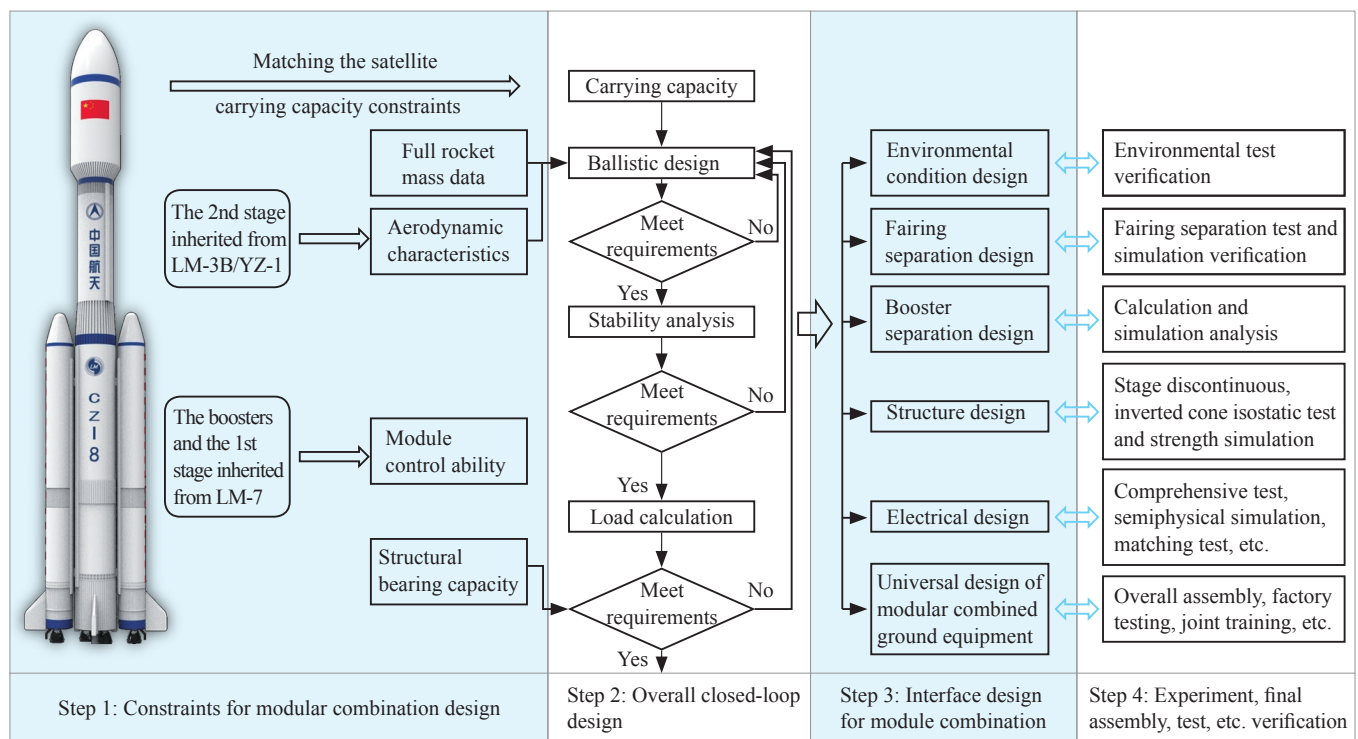

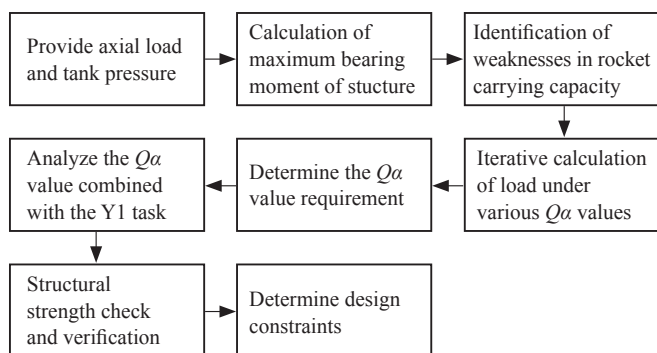Figure 5 Development process based on modular combination

Figure 6 The process of determining the $Q\alpha$ value

Table 3 Maximum flight overload of domestic launch vehicle

No.	Launch vehicle	Maximum flight overload (g)	Satellite's weight (t)
1	LM-2C	6.6−6.7	1
2	LM-2F	5	8
3	LM-3B	5.3	5
4	LM-3A	5	3
5	LM-3C	5.3	4
6	LM-7	5.3	12
7	LM-5	5.5	8
8	LM-5B	5.8	20
9	LM-4C	5.3	3
10	LM-6A	5	4.5

and LM-2D are in the 1 t level. For 3 t, 4.5 t or even heavier satellites, the maximum overload of China's launch vehicles is maintained at 5.3−5.8 g. Therefore, the maximum overload of LM-8 during flight was set to be within 6 g.

3.1.2 Overall closed-loop design that satisfied the design conditions for capacity, overload and load

LM-8 uses technologies such as engine throttling, a wind compensation trajectory design, and active load shedding to meet the $Q\alpha$ value constraint requirements. The specific content can be seen in section 3.4.

3.1.3 Environmental adaptability based on module combination

There were adaptability issues due to inheriting modules in different flight environments. Therefore, it was necessary to analyze the entire flight profile and determine the appropriateness

of the environmental conditions. At the same time, checking the mechanical and thermal environment adaptability of all the modules. Modules that could not meet the requirements of the new environment required supplemental test verification. Although the first-stage module was inherited, the working environment of the engine rack was changed due to the engine throttling requirement and the reduction of two side boosters, etc. The adaptability was verified by mechanical simulation as shown in Figure 7.
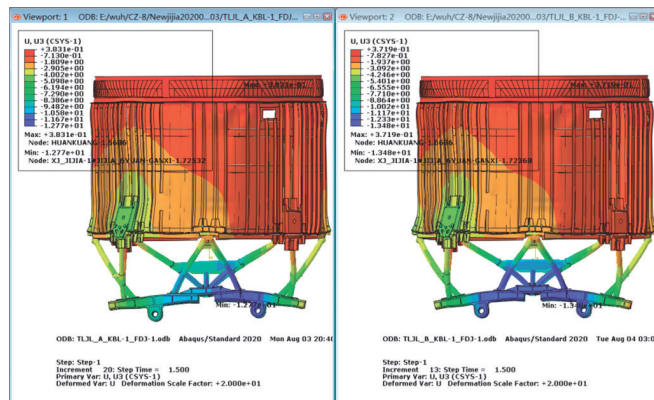

Figure 7 The mechanical simulation of the engine rack

3.1.4 Module interface design

The module interface design of each system was carried out as part of the entire research and development process. Inheriting existing modules as much as possible in the design, while concentrating on the limiting modules or items that must be changed. In view of the impact of interface changes, the separation design and pressurization scheme verification were carried out to ensure flight safety. The fairing was composed of two parts, which were verified by separation simulation and separation experiment as shown in Figure 8.
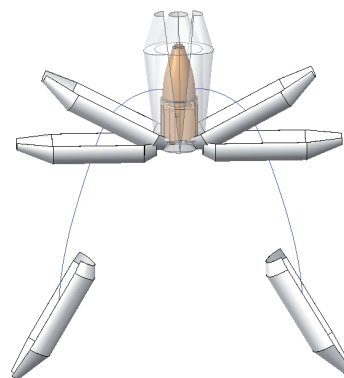

Figure 8 Separation simulation of fairing

3.1.5 Test verification and flight conditions

The modified modules were fully simulated and verified by ground tests, then the final assembly, tests, refueling and flight test were completed at the launch site. The interfaces between the modules were well matched, the flight process was in normal state, and actions such as separation and pressurization were completed as expected, which indicated that the module combination design was reasonable and correct.

3.2 Engine Thrust Regulation

LM-8 conducts thrust regulation with the engine during flight, and was first time this was applied in China's launch vehicles. This technology greatly improved the overall design optimization capability and enhanced the launch vehicle's mission adaptability. In addition, the use of engine thrust regulation enabled the relevant technical verification in advance for the subsequent reusable technology of China's expendable launch vehicles, and laid a solid foundation for the development of China's reusable launch vehicles.

3.2.1 Realization of thrust regulation

The high-thrust liquid oxygen/kerosene engine system is equipped with a flow regulator in the fuel supply path of the gas generator. As shown in Figure 9, when the thrust needs to be regulated, the engine assembly of the flow regulator is rotated to reduce the opening of the flow regulator, so that the fuel flow and the combustion temperature of the generator are reduced. In turn, the output power of the turbine and the flow of liquid oxygen and kerosene into the engine are also reduced, realizing engine thrust regulation in flight.
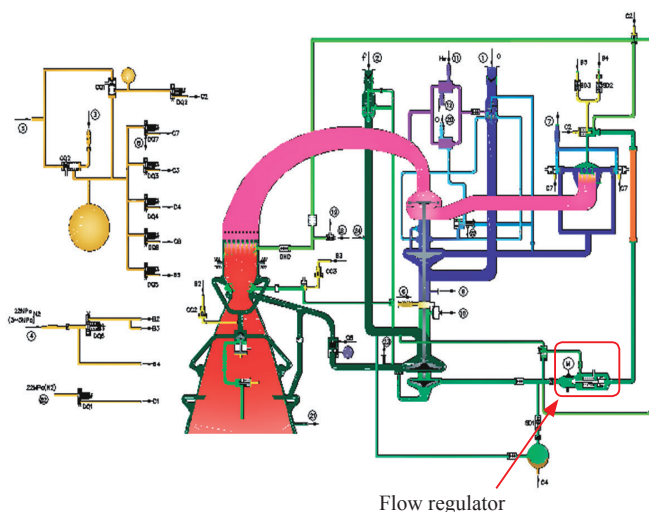
3.2.2 Development of engine adaptability

Engines work over a long-time low-operation conditions so that it is necessary to improve their adaptability, including engine structural layout adaptability, low-operation condition operation adaptability, engine performance under low-operation conditions, as well as the characteristics of the evaporator and the matching between engine components and measurement and control cables. In addition, there was a risk that the residual axial force of the turbo oxygen pump would increase. An operation load test was set up to validate operation under low-operation conditions.

3.2.3 Adaptability improvement of control system

The control system adopts a thrust regulating engine control matching test to verify the frequency conversion control law and the matching relationship between the drive circuit and the stepper engine. The first stage servo mechanism adaptively adjusts the low operation condition of the engine, and completed a performance verification test under high pressure and low pressure drainage conditions, demonstrating the variable thrust condition of the engine.

3.2.4 Effectiveness analysis

Three tests were completed on the ground, enabling the operational stability and compatibility of the engine and control system to be assessed. The net adjustment conditions in flight were stable and consistent with expectations. As shown in Figure 10, the engine's parameters were stable during the thrust adjustment process.
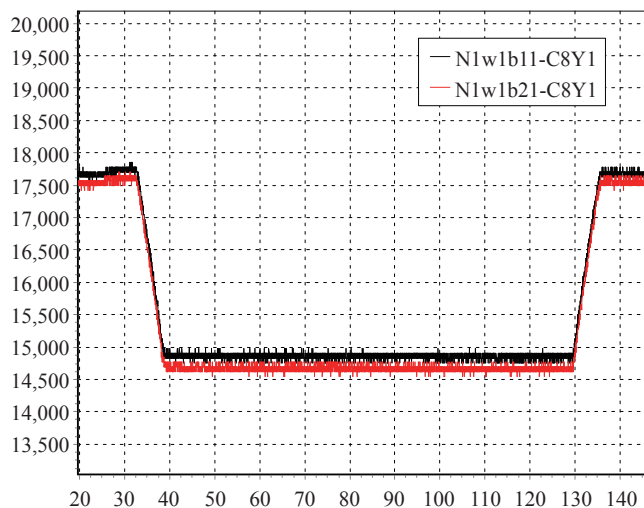

Flow regulator

Figure 9 Schematic diagram of engine flow regulation

Figure 10 The engine's parameters during the thrust adjustment process

3.3 Modal Parameter Acquisition Technology Based on Numerical Simulation

LM-8 was the first medium-lift strap-on launch vehicle developed without an integrated modal test in China. Based on the test data and structural dynamic model of the existing modules, the modal parameters of the launch vehicle were obtained by assembly of the existing structural dynamic models and numerical simulation. The research and development of LM-8 has laid the technical foundation for the development of other larger and heavier launch vehicles to have a shorter development cycle and reduced development cost.

Because most modules of LM-8 were inherited from other mature launch vehicles whose structural dynamic models were modified by modal tests and verified by flight tests, only part of the structures needed to be redesigned. Therefore, the key influence factor of the modal parameters was the accuracy of the modules' connection modeling and the predictive accuracy of local mode slope. The LM-8 team proposed a technical scheme based on the combination of the existing module modal test data and numerical simulation analysis to obtain the modal parameters of the launch vehicle. In addition, a modal parameter deviation selection method was adopted based on the sensitivity analysis of the key segment connection stiffness, and the refined prediction technology of the local mode slope was first applied. In order to obtain the modal parameters of the launch vehicle quickly and accurately, operations in five aspects were carried out, including fine structure dynamic modeling and model assembly, sensitivity analysis of key segment connection stiffness, fine simulation prediction of the local mode slope of inertial unit installation position, modal test data and deviation statistical envelopment analysis of similar models, and verification of the vertical modal test at the launch site. The technical route for obtaining the modal parameters of the complete launch vehicle is shown in Figure 11.

In order to verify the accuracy of the technical scheme, a simple modal test in its vertical state was carried out at the launch site.

The test results and simulation analysis results are listed in Table 4.
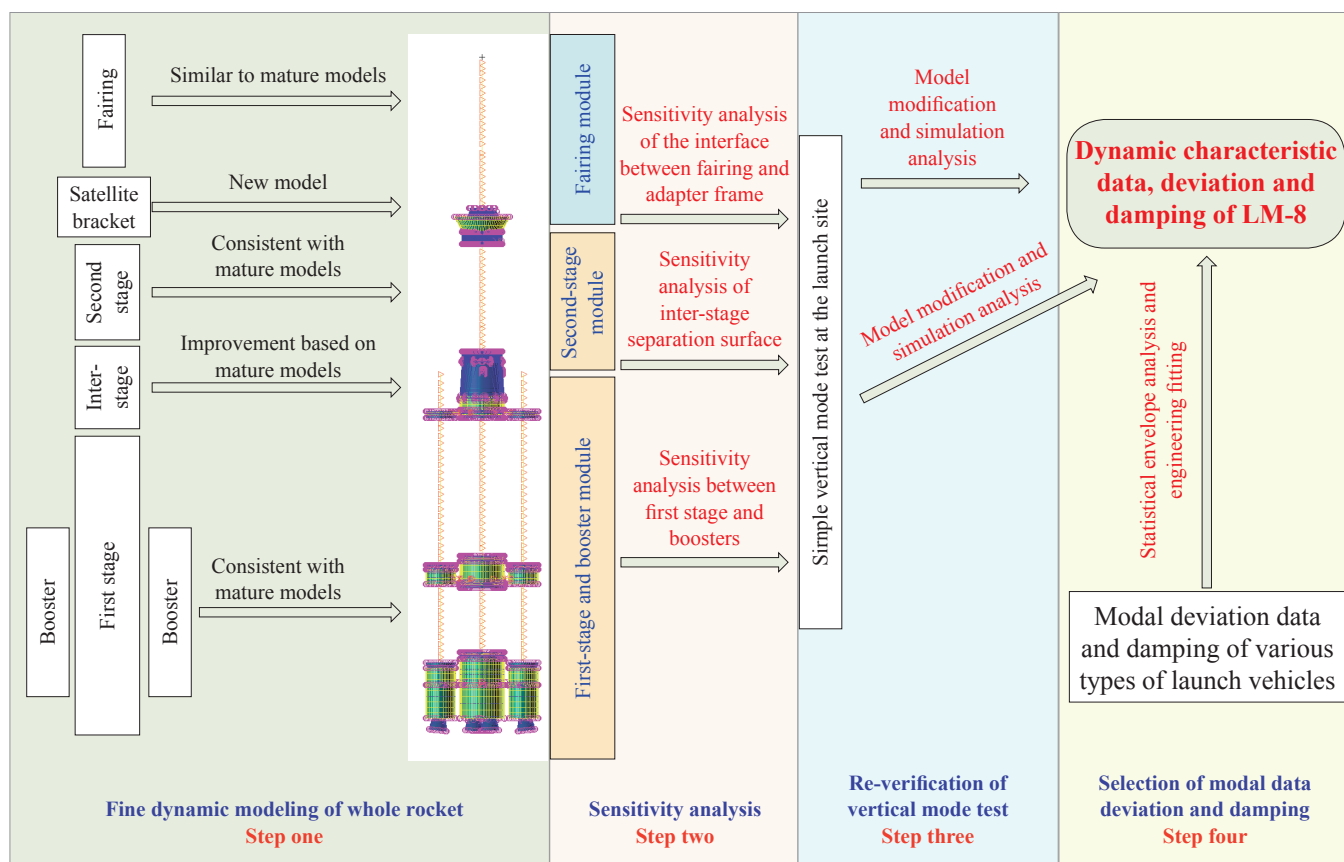
The results showed that the deviation between the test
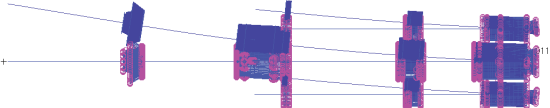

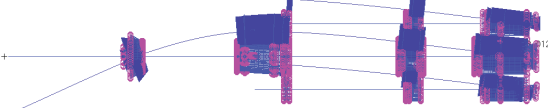Figure 11 LM-8 dynamic characteristic acquisition technology roadmap

Table 4 Comparison of test and simulation results

Simulation analysis results		Relative deviation of frequency between test and simulation
	First order Z-direction frequency	0.0%
	First order Y-direction modal shape	3.7%
	First order Z-direction frequency modal shape	2.4%
	Second order Y-direction frequency modal shape	3.2%

a) The relative deviation between the test value of the transverse first-order modal frequencies and the results of numerical simulation analysis was 0%−3.7%;

b) The relative deviation between the test value of the transverse second-order modal frequencies and the results of numerical simulation analysis was 2.4%−3.2%;

c) The deviation between the simulation value and the test value of the velocity gyro position modal slope was −0.006 (transverse second-order Z-direction) and −0.004 (transverse second-order Y-direction), respectively.

values and the simulation results was small, which indirectly verified the accuracy of the structure dynamic model. In the actual flight process, the attitude control of the launch vehicle was stable, which also indirectly indicated that the modal parameters of the launch vehicle were in line with the design, and the design was accurate.

3.4 Onboard Load Relief Control Technology

Since LM-8 inherited existing modules from other launch vehicles, the load capacity was severely limited. After iterative optimization of trajectory, control system, and load design, the flight loads did not exceed the load capacity. Several technologies were adopted to reduce the flight loads, including engine throttling, wind compensation design, and load relief control. It is worth mentioning that it was the first time the effect of load relief control was taken into consideration during the pre-launch "Go/No go" phase. The flight loads were reduced significantly, and the load relief control technologies were well matched, which satisfied the load capacity of the structure.

In the traditional forward design, the maximum flight $Q\alpha$ value would exceed the load capacity considerably, and the flight

overload would be 6.9 g.

The relationship of load relief and wind compensation is illustrated in Figure 12, and the principle of combination with load relief and wind compensation is illustrated in Figure 13.
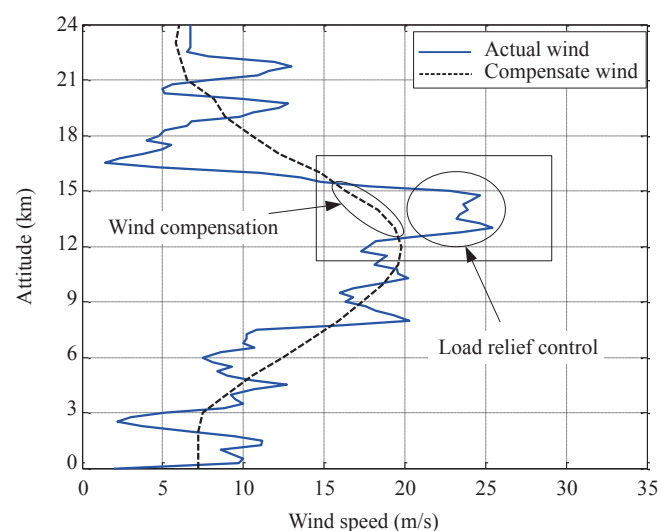

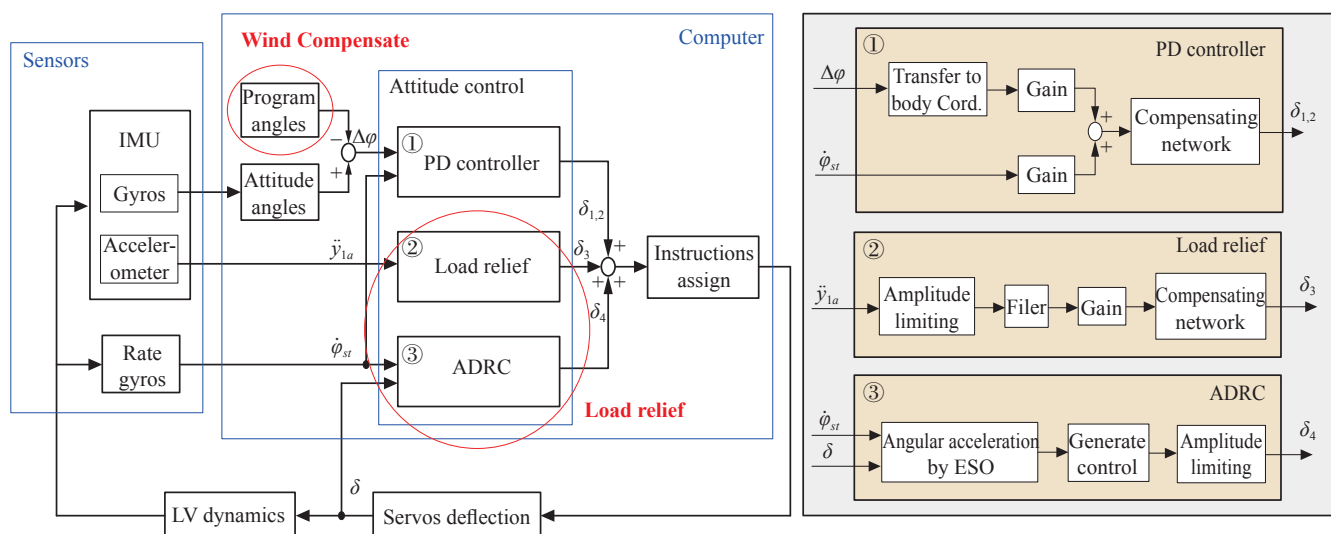Figure 12 Relationship of load relief and wind compensation

Figure 13 Principle of combination with wind compensation and load relief

3.4.1 Analysis of trajectory design based on engine throttling

After analyzing various factors such as different throttling capacities and throttling period, it was concluded that the deeper the engine throttling ability is, the more effective to reduce the maximum dynamic pressure. In addition, the earlier the throttling period is, the more effective to reduce the maximum dynamic pressure, meanwhile the greater loss of capacity. Relying on the throttle trajectory alone, the dynamic pressure could be reduced by up to 10% for the mission profile as shown in Figure 14, but it still could not meet the total load limits.
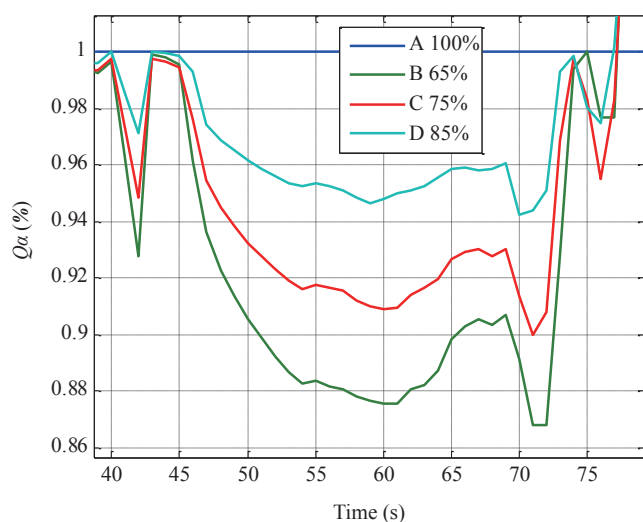

Figure 14 $Q\alpha$ reduction is different for different engine adjustment depths.

3.4.2 Wind compensation trajectory design

A two-channel wind compensation trajectory design was adopted, and 4 trajectories were obtained according to different scenarios. The maximum $Q\alpha$ value was further reduced by up to 10%, but still couldnot meet the total load limits.

3.4.3 Load relief control design

LM-8 adopted onboard load relief control technology based on lateral acceleration measured by the inertial measurement unit (IMU), which was installed in the instrument bay.

The IMU accelerometer measurement was sensitive to attitude angular acceleration and elastic vibration. Taking the pitch channel as an example, the IMU accelerometer measurement equation can be expressed as Equation (1).

$$\ddot{y}_{1a} = \ddot{y}_1 + \underline{l_{ax}\Delta\ddot{\varphi}} + \sum_i \left[U_{yi}(x_a)\ddot{q}_i + n_x g_0 R_{zi}(x_a)q_i \right] \tag{1}$$

where $\ddot{y}_1$ is the parent acceleration of mass center in body coordinate system, l_{ax} is the distance from IMU accelerometer to mass center, $\Delta\ddot{\varphi}$ is pitch angular acceleration, $U_{yi}(x_a)$ and $R_{zi}(x_a)$ represent the i-th order mode and mode slope in accelerometer position, q_i is the i-th order mode generalized operator, $n_x g_0$ is the axial acceleration.

The effect of elastic vibration was suppressed by the filter network, and the effect of attitude angular acceleration was compensated with ADRC by observing the signal of rate gyros.

With the combination of engine throttling, wind compensation trajectory design and load relief control, the maximum $Q\alpha$

value was reduced to meet the design requirements.

3.4.4 Analysis of performance

According to the flight telemetry data and the actual wind measured half an hour after launch, the flight $Q\alpha$ was identified. At the same time, the aerodynamic and structural disturbances were identified through multiple flight simulations.

A six degree-of-freedom dynamic model was adopted for simulation, the translational motion was described as Equations (2) and (3).

$$\begin{bmatrix} \dot{X} \\ \dot{Y} \\ \dot{Z} \end{bmatrix} = \begin{bmatrix} V_x \\ V_y \\ V_z \end{bmatrix} = \begin{bmatrix} V\cos\theta\cos\sigma \\ V\sin\theta\cos\sigma \\ -V\sin\sigma \end{bmatrix} \quad (2)$$

$$\begin{bmatrix} m\dot{V} \\ mV\dot{\theta}\cos\sigma \\ -mV\dot{\sigma} \end{bmatrix} = H_B \begin{bmatrix} 2P_{xj} + 2P_{zt} \\ -P_{xj}\delta_{xj} + P_{xj}\delta_{xj4} \\ -(-P_{xj}\delta_{xj1} + P_{xj}\delta_{xj3} - P_{zt}\delta_{zt1} + P_{zt}\delta_{zt3}) \end{bmatrix}$$

$$+ H_V \begin{bmatrix} -C_x qS_m \\ C_y^\alpha qS_m(\alpha+\alpha_W) \\ -C_z^\beta qS_m(\beta+\beta_W) \end{bmatrix} + mH_G \begin{pmatrix} g_x \\ g_y \\ g_z \end{pmatrix} - mH_G \begin{bmatrix} a_{11} & a_{12} & a_{13} \\ a_{21} & a_{22} & a_{23} \\ a_{31} & a_{32} & a_{33} \end{bmatrix} \quad (3)$$

$$\begin{bmatrix} X + R_{0x} \\ Y + R_{0y} \\ Z + R_{0z} \end{bmatrix} - mH_G \begin{bmatrix} b_{11} & b_{12} & b_{13} \\ b_{21} & b_{22} & b_{23} \\ b_{31} & b_{32} & b_{33} \end{bmatrix} \begin{bmatrix} \dot{X} \\ \dot{Y} \\ \dot{Z} \end{bmatrix} - H_B \begin{bmatrix} 0 \\ F_{by} \\ -F_{bz} \end{bmatrix}$$

where $\begin{bmatrix} \dot{X} \\ \dot{Y} \\ \dot{Z} \end{bmatrix}$ is the position in launch coordinate, $\begin{bmatrix} V_x \\ V_y \\ V_z \end{bmatrix}$ is the velocity in launch coordinate, V is the velocity, θ is trajectory inclination angle, σ is track yaw angle, α is the angle of attack, β is the angle of sideslip, α_w is the angle of attack caused by wind, β_w is the angle of sideslip caused by wind, C_y^a is the lift coefficient, C_z^β is the side force coefficient, m is the mass of launch vehicle, p_{xj} is the thrust of core engine, p_{zt} is the thrust of booster engine, q is the dynamic pressure, S_m is the reference area, F_{by}, F_{bz} is the disturbing force coefficient, $\begin{bmatrix} g_x \\ g_y \\ g_z \end{bmatrix}$ is the gravity projected in launch coordinate, $\begin{bmatrix} \omega_{ex} \\ \omega_{ey} \\ \omega_{ez} \end{bmatrix}$ is the Earth's rotation speed in launch coordinate, H_V is the coordinate transformation matrix of velocity coordinate to half velocity coordinate, H_B is the coordinate transformation matrix of body coordinate to half veloc-

ity coordinate, H_G is the coordinate transformation matrix of launch coordinate to half velocity coordinate.

The rotational motion is described as:

$$\begin{bmatrix} J_{x1} & 0 & 0 \\ 0 & J_{y1} & 0 \\ 0 & 0 & J_{z1} \end{bmatrix} \begin{bmatrix} \dot{\omega}_{Tx_1} \\ \dot{\omega}_{Ty_1} \\ \dot{\omega}_{Tz_1} \end{bmatrix} = \begin{bmatrix} \omega_{Ty_1}\omega_{Tz_1}\left(J_{y1}-J_{z1}\right) \\ \omega_{Tx_1}\omega_{Tz_1}\left(J_{z1}-J_{x1}\right) \\ \omega_{Tx_1}\omega_{Ty_1}\left(J_{x1}-J_{y1}\right) \end{bmatrix}$$

$$- \begin{bmatrix} P_{xj}\left(\delta_{xj1}+\delta_{xj2}+\delta_{xj3}+\delta_{xj4}\right)Z_{rxj}/\sqrt{2} + P_{zt}\left(\delta_{zt1}+\delta_{zt3}\right)Z_{rzt} \\ P_{xj}\left(-\delta_{xj1}+\delta_{xj3}\right)\left(X_{rxj}-X_z\right) + P_{zt}\left(-\delta_{zt1}+\delta_{zt3}\right)\left(X_{rzt}-X_z\right) \\ P_{xj}\left(-\delta_{xj2}+\delta_{xj4}\right)\left(X_{rxj}-X_z\right) \end{bmatrix} \quad (4)$$

$$- \begin{bmatrix} 0 \\ C_n^\beta qS_m\left(X_y-X_z\right)(\beta+\beta_W) \\ C_n^\alpha qS_m\left(X_y-X_z\right)(\alpha+\alpha_W) \end{bmatrix} - \begin{bmatrix} m_{dx}qS_m l_k^2/V\omega_{x_1} \\ m_{dy}qS_m l_k^2/V\omega_{y_1} \\ m_{dz}qS_m l_k^2/V\omega_{z_1} \end{bmatrix} + \begin{bmatrix} M_{bx} \\ M_{by} \\ M_{bz} \end{bmatrix}$$

where J_{x1}, J_{y1}, J_{z1} are the rotational inertia of axis x_1, y_1, z_1 respectively, $\omega_{Tx}, \omega_{Ty}, \omega_{Tz}$ are the rotational angular velocity of x_1, y_1, z_1 axis respectively, $\delta_{xj1,2,3,4}$ is the engine deviation, X_z is the mass center coordinate, X_y is the pressure center coordinate, X_{rxj} is the engine position coordinate, $C_n^{\alpha,\beta}$ is the normal force coefficient, m_{dx}, m_{dy}, m_{dz} are the damping moment coefficient of axis x_1, y_1, z_1, M_{bx}, M_{by}, M_{bz} are the disturbing moment coefficient.

As shown in Figure 15, the blue line is the $Q\alpha$ curve calculated from telemetry data, and the red dotted line is the simulated $Q\alpha$ curve. The simulation results match the telemetry results well, indicating that the flight load control technology was applied successfully.
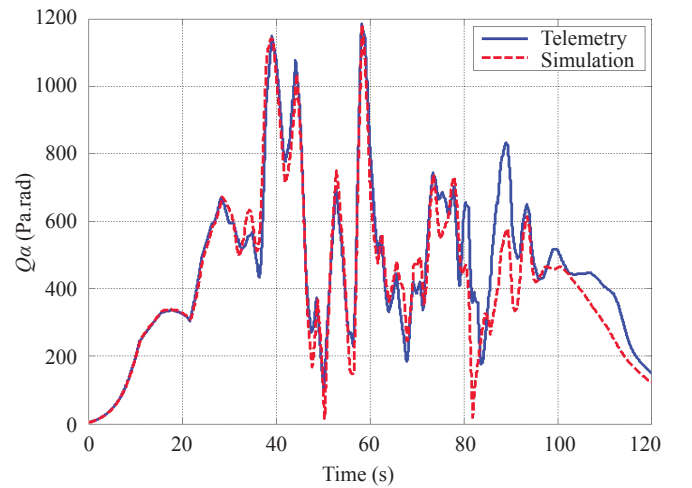

Figure 15 Simulation results and the telemetry identification results

4 DEVELOPMENT PROSPECTS

4.1 Upgrade 3.35 m Oxygen/hydrogen Module to Improve Mission Performance

With the increase of payload demand, the carrying capacity and the fairing envelope space are constantly increasing. The current state of the fairing diameter cannot meet the requirements, and the carrying capacity of the second stage is limited, which also restricts the development and application of the launch vehicle. In the future, a 3.35 m diameter oxygen/hydrogen module will be adopted, which can adapt to a 5.2 m diameter fairing to meet the requirements of larger satellites. The load-bearing capacity of structures will be increased, improving the launch capability and enhancing mission adaptability. The larger carrying capacity will further improve the efficiency for satellite networking.

4.2 Adopt Integrated, Rapid Measurement and Launch Technologies to Implement Efficient and Low-cost Launches

In order to meet the commercial launch market's requirements of high-efficiency and low-cost launches [6], the LM-8 development has achieved a number of technological innovations, including electrical integration, ground-based test and launch control, launch and control integration, rapid structural manufacturing, and rapid measurement, reduced launch costs and improved manufacturing efficiency. LM-8 will optimize the mission process and reduce the operations of the launch site, including the implementation of product loading and transportation, three-level testing and launching, automated testing, and effectively shorten the launch cycle.

4.3. Innovative practice and become a test case for reusable and other new technologies

LM-8 maintains an open and innovative platform, striving to become a test case for verification of new technologies. New technologies will be continuously used to improve flight reliability, including the use of autonomous technology to improve the ability to avoid failures such as thrust drops [7], the use of take-off drift active control technology [3] to ensure the safety of the take-off tower process, the use of "no window constraints" self-correcting guidance and control technology to meet the requirements of multi-constraint high-precision orbit insertion. LM-8 will also carry out the exploration for reusing related technologies in flight, including guidance and control algorithm verification, re-entry environment acquisition, thermal protection material loading to accumulate experience for reuse engineering applications.

REFERENCES:

[1] Satellite manufacturing and launch systems market—growth, trends, and forecast (2019-2024) [R]. Mordor Intelligence Pvt Ltd, 2019.01.

[2] WANG X J, FAN R X, CHENG T M, et al. Maiden flight of Long March 7—the new generation medium launch vehicle in China [J]. Aerospace China, 2016, 17(3):12−18.

[3] SONG Z Y, WU Y T, XU S S, et al. LM-8: the pioneer of Long March rocket series on the innovations of commercialization and intelligence [J]. Journal of Deep Space Exploration, 2021(1):1−13.

[4] LU Y. Space launch vehicle's development in China [J]. Astronautical Systems Engineering Technology, 2017, 1(3):1−8.

[5] LONG L H. Development prospects for Chinese launch vehicles [J]. Aerospace Manufacturing Technology, 2010(3):5−10.

[6] WANG X J. The development and future of China's commercial aerospace [J]. Astronautical Systems Engineering Technology, 2020(01):1−6.

[7] SONG Z Y, WANG C, GONG Q H. Autonomous trajectory planning for launch vehicle under thrust drop failure [J]. Sci Sin Inform, 2019, 49(11): 1472−1487.

Author Biography:

CHEN Xiaofei (1987−), senior engineer, graduated from the School of Aerospace Engineering, Tsinghua University with a Master's degree. Now he is working at the Beijing Institute of Astronautical Systems Engineering, engaged in the overall design of liquid launch vehicles.

Corresponding Author:

SONG Zhengyu, a researcher at the China Academy of Launch Vehicle Technology, the chief designer of the LM-8 launch vehicle.